Essays Biochem. (2010) **47**, 1–23; doi:10.1042/BSE0470001

1

The mitochondrial respiratory chain

Peter R. Rich[1] and Amandine Maréchal

Glynn Laboratory of Bioenergetics, Department of Structural and Molecular Biology, University College London, Gower Street, London WC1E 6BT, U.K.

Abstract

In the present chapter, the structures and mechanisms of the major components of mammalian mitochondrial respiratory chains are reviewed. Particular emphasis is placed on the four protein complexes and their cofactors that catalyse the electron transfer pathway between oxidation of NADH and succinate and the reduction of oxygen to water. Current ideas are reviewed of how these electron transfer reactions are coupled to formation of the proton and charge gradient across the inner mitochondrial membrane that is used to drive ATP synthesis. Additional respiratory components that are found in mammalian and plant, fungal and algal mitochondria are also reviewed.

Introduction

Mitochondria are organelles that are found in most eukaryotic cells. In mammals, they are present in all cell types apart from anucleate red blood cells. Most cells contain very many mitochondria, with the largest numbers (more than 10^4) in those with the highest energy requirements. In extreme cases, for example in hummingbird flight muscle, mitochondria can constitute 35% of the cell volume. Typically, mitochondria are rod-shaped with a diameter of approx. 1 μm. However, their shapes and sizes can vary considerably, and in some types of cells they instead appear as a contiguous reticulated network.

[1]*To whom correspondence should be addressed (email prr@ucl.ac.uk).*

Mitochondria within a cell also appear to move along microfilaments and to be in a constant state of fission and fusion. The significance of such morphological differences and dynamic behaviour is still not well understood.

Mitochondria are thought to have evolved at least 2000 million years ago from bacteria that had acquired an oxygen-utilizing respiratory chain in response to the increasing levels of atmospheric oxygen that arose from the advent of oxygenic photosynthesis [1]. These oxygen-utilizing bacteria were, most probably, similar to present-day α-proteobacteria and initially formed a symbiotic relationship with, and were engulfed by, another type of bacterial or primitive eukaryotic cell. This was followed by a gradual transfer of most of the genes into the host cell nucleus, where they were better integrated with the other cellular processes and controls, resulting in the present-day non-autonomous mitochondrial organelles. Many features of mitochondria, including their shapes and overall structures, reflect their bacterial origin. Particularly convincing is the fact that they retain some of their original DNA. This mtDNA (mitochondrial DNA) still exhibits clear bacterial features [2]. In humans, for example, the mtDNA is a closed-circular, double-stranded structure, forming a very compact 16569 bp genome which encodes 37 genes. These include genes for 22 tRNAs (transfer RNAs) and two rRNAs (ribosomal RNAs). Together with a range of nuclear-encoded factors, they provide the mitochondria with its own replication, translation and transcription system. This is governed by a different genetic code from that of the nucleus and retains many features that are more akin to bacterial systems. The other 13 mtDNA genes encode proteins that are synthesized within the mitochondria and all are integral components of respiratory chain complexes or ATP synthase.

Mitochondria possess two phospholipid membranes that result in four biochemically distinct compartments [3]. The outer membrane forms the boundary with the cytoplasm. It is permeable to small molecules and has specific proteins to facilitate inward transfer of cytoplasmically synthesized mitochondrial proteins. It is also the site of many other specific biochemical functions, including a set of poorly understood processes that can trigger release of mitochondrial components into the cytoplasm that then induce cellular apoptosis [4]. Inside it is the IMM (inner mitochondrial membrane). The IMS (intermembrane space) between the two membranes is also biochemically distinct and contains, for example, those proteins that are released into the cytoplasm when apoptosis is triggered. Remarkably, one of these proteins, cytochrome *c*, is also a key component of the respiratory electron transfer chain. All other proteins that comprise the four major respiratory chain complexes are assembled into distinct multiprotein structures that span the IMM. The IMM also hosts the ATP synthase; one part spans the IMM and is connected to large catalytic domains that project into the matrix space within the IMM. The IMM is usually highly invaginated in order to increase its surface area so that it can house the vast numbers of respiratory chains and ATP synthases that are needed to produce the power that cells and organisms require;

for example, an average human requires approx. 100 W of basal power to survive [5] and most of this comes from the mitochondrial ATP that is produced by the IMM proteins. The matrix space within the IMM is very densely packed with cytoplasmically derived metabolic enzymes, such as those required for the TCA (tricarboxylic acid) cycle (also called the citric acid cycle), amino acid metabolism and urea synthesis. It also contains multiple copies of mtDNA, together with the machinery for its replication, translation and transcription.

Modern-day mitochondria are composed of thousands of different types of proteins, the vast majority nuclear-encoded, that perform a very wide range of metabolic functions. In the present chapter we focus on the respiratory electron transfer chain and the ways in which it derives energy from oxidation of metabolic products of food assimilation to produce a PMF (protonmotive force) that drives ATP synthesis.

Coupling between respiration and ATP synthesis

Respiratory electron transfer and the energy-requiring process of phosphorylation of ADP to produce ATP are not directly coupled to each other within the same enzyme complex. Instead, they are linked indirectly through a PMF that is generated across the IMM by the activity of the electron transfer chain [6]. The electron transfer reactions are exergonic and would produce heat if they occurred in a simple solution. However, the protein complexes are embedded in the IMM with their reaction sites spatially organized in a very precise 'vectorial' manner. As a result, the electron transfers result in both charges and protons being moved across the IMM, generating the PMF that is composed of a pH gradient (more acidic outside) and an electrostatic charge difference (positive outside). Hence, the potential energy released by electron transfer is retained in this charge and proton gradient and can be used subsequently to drive the synthesis of ATP via the ATP synthases.

Aerobic glucose oxidation begins with glycolysis in the cytoplasm, yielding two NADH, two ATP and two molecules of pyruvate. The pyruvates are transported into the mitochondrial matrix where their acetyl groups are transferred to CoA by pyruvate dehydrogenase with formation of two NADH. The acetyl groups of the two acetylCoA products are transferred on to oxaloacetates and hence enter the TCA cycle where they are oxidized to CO_2 and water. This yields six NADH and two GTP. The NADH produced by glycolysis and the TCA cycle, together with the succinate intermediate of the TCA cycle, are electron-rich substrates that are oxidized by the respiratory chain complexes I and II respectively. These in turn pass the electrons to UQ (ubiquinone), a small, lipid-soluble organic molecule that can be reduced and oxidized, and can freely diffuse within and across the IMM. The reduced UQ [UQH_2 (ubiquinol)] diffuses to complex III where it is reoxidized. Complex III reduces the IMM-located cytochrome *c*, which in turn reduces complex IV

where oxygen is reduced to water. This chain of electron transfers provides the potential energy that powers the generation of the PMF and, hence, the formation within the matrix of ATP from ADP and phosphate. ADP and phosphate are driven into the matrix, and ATP out to the IMS (and hence to the cytoplasm), by some of the energy of the PMF. By taking into account the number of protons/charges transferred by electron transfer and the numbers required for ATP synthesis and substrate (pyruvate, ADP and P_i) and product (ATP) exchanges across the IMM, yields of ATP can be calculated. Oxidation of glucose to pyruvate results in the generation of two ATP directly and a further six from the NADH that is transferred to the matrix. A further approx. 22 ATP are produced from the aerobic oxidation of pyruvate to CO_2 and water within the mitochondria [7]. Hence, the addition of aerobic mitochondrial respiration to glycolysis greatly increases the efficiency of glucose oxidation and the resultant yield of ATP.

The respiratory chain

Figure 1 provides an overview of topographical and atomic resolution information on the four major mammalian respiratory complexes and ATP synthase. The information has been derived from electron microscopic imaging of individual electron transfer complexes and from high-resolution X-ray crystallography of three-dimensional crystals. These structural data,

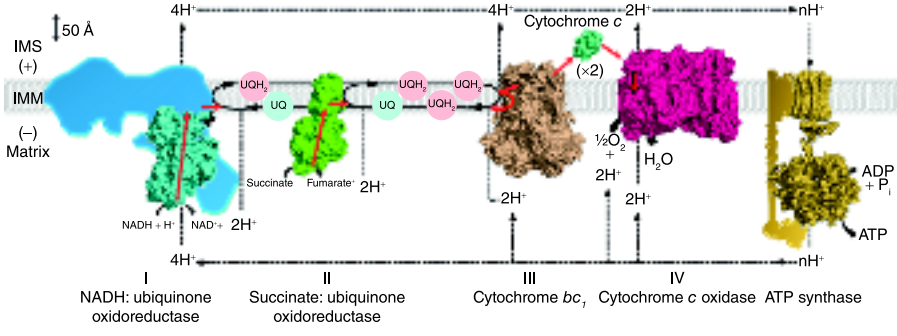

Figure 1. An overview of the respiratory chain and ATP synthase

Complexes are scaled to a 50 Å IMM. Red arrows represent the transfer of the two electrons produced by the oxidation of NADH or succinate by complex I or II respectively. These electrons are transferred to complex III via the pool of UQ and then to complex IV via soluble cytochrome *c*. Details of the proton circuit that drives ATP synthesis are described in the text. The number of protons, *n*, required to form ATP is dependent on the number of c subunits in the membrane segment of ATP synthase. Yeast mitochondria have ten c subunits. Hence, passage of ten protons will cause one complete rotation of the rotor and formation of three ATP, giving a value for *n* of 3.33 (see the ATP synthase chapter in this volume for further details). The protein complexes were drawn using PyMOL (DeLano Scientific; http://www.pymol.org). PDB files were: 2FUG, hydrophilic domain of complex I from *Thermus thermophilus* at 3.3 Å [11]; 1ZOY, porcine complex II at 2.4 Å [14]; 1BGY, dimeric bovine complex III at 3.0 Å [34]; 2B4Z, bovine cytochrome *c* at 1.5 Å [35]; 2OCC, dimeric bovine complex IV at 2.3 Å [36]; 1QO1, yeast ATP synthase at 3.9 Å [37].

together with a vast amount of information from other spectroscopic methods, have led to understanding of many details of the electron and proton transfer mechanisms involved. For simplicity, the Figure shows one of each major complex and they are described individually below; however, their real organization is very different. For example, the relative amounts of complexes vary enormously in mitochondria from different organisms and even between different tissues in the same organism. There is also increasing evidence that the complexes can associate together in specific combinations to form well-defined 'supercomplexes' [8] and, most probably, that the components are not homogeneously distributed throughout all areas of the same IMM.

Complex I (NADH:UQ oxidoreductase)

NADH from glycolysis is transferred into the matrix by a 'substrate-shuttle' mechanism. This, together with the matrix NADH produced by the TCA cycle, is reoxidized to NAD^+, coupled to reduction of membrane-located UQ, by NADH:UQ oxidoreductase. Although different types of NADH:UQ oxidoreductase can be found in fungal, algal and plant mitochondria (see below), mammalian mitochondria possess only complex I. Electron transfer within complex I is coupled to proton translocation across the IMM, greatly increasing the efficiency of NADH oxidation and, hence, the ultimate yield of ATP.

Structure

Bovine complex I consists of 45 different subunits with a combined mass of ~980 kDa [9]. Bacterial forms of complex I are smaller (~500 kDa), typically consisting of just 14 subunits that appear to form a minimal common catalytic core. Electron microscopy of single particles of complex I from all sources reveals an L-shaped structure [10]. It is thought that one arm is hydrophobic and embedded across the IMM and the other is hydrophilic and projects into the matrix (Figure 1). In mammalian systems, seven of the core subunits are encoded by mtDNA and located in the hydrophobic arm.

An X-ray crystal structure of the hydrophilic domain of complex I of the thermophilic bacterium *Thermus thermophilus* [11] has defined the positions of known redox cofactors (Figure 2). Some of these can be equated to iron–sulfur (Fe–S) centres that had been identified previously by EPR spectroscopy. The cofactors are a non-covalently bound FMN (flavin mononucleotide), two [2Fe–2S] Fe–S centres (EPR-detected signals N1a and N1b) and six [4Fe–4S] Fe–S centres (EPR-detected signals N2, N3, N4, N5, N6a and N6b). A ninth [4Fe–4S] Fe–S centre (labelled N7 in Figure 2) is also present in this bacterial structure, but is not found in mitochondrial complex I. Centre N1a is close to FMN but is separate from the main electron transfer pathway and its function is still not clear. The binding site for NADH is close to FMN and it is evident that the Fe–S centres (apart from N1a and N7) form a pathway for transferring electrons from FMN towards the interface of the hydrophilic and membrane arms. This chain

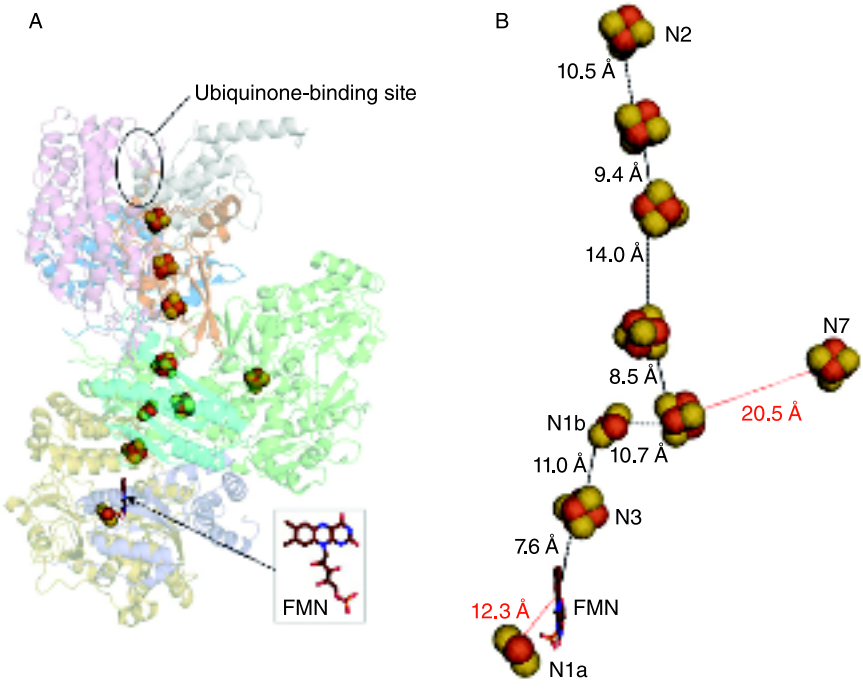

Figure 2. Structure of complex I and its prosthetic groups
(**A**) Overall structure of the hydrophilic domain of bacterial complex I from *Thermus thermophilus* at 3.3 Å (PDB: 2FUG) [11]. Different colours have been used to highlight different subunits. (**B**) Electron transfer cofactors. Edge-to-edge distances between the prosthetic groups are shown in black. Other distances are shown in red.

probably starts with centres N3 and N1b, which are close to the FMN, and ends with centre N2, which is closest to the UQ-binding site. The four [4Fe–4S] centres between these are not labelled in Figure 2 because their correspondence to specific EPR-detected signals N4–N6 is not fully resolved.

There is increasing evidence that this very large complex has evolved from smaller, pre-existing modules [12]. For example, three protein subunits of the hydrophilic arm house the NADH-binding site, FMN, Fe–S centres N3, N1b and three other Fe–S centres. These three subunits have homology with the NADH oxidoreductase fragment of an NAD^+-reducing hydrogenase. Other domains may have arisen from additional types of precursor enzymes. Some subunits of the hydrophobic arm show weak homologies with Na^+/H^+ antiporters, although the significance of this remains obscure and, most surprisingly, it appears most likely that none contain detectable redox centres.

Mechanism

The internal redox reactions involve electron transfer from NADH, via FMN, through a linear series of Fe–S centres to N2, the Fe–S centre with the highest redox potential and the one likely to be the immediate donor to substrate

UQ. Although the location of the UQ-binding site (and even the number of such sites) remains in dispute, it must be close to centre N2. Centre N2 itself is expected to be very close to the membrane interface [11], although some studies suggest that it is more than 30 Å (1 Å=0.1 nm) away, with a connecting channel from the membrane through which UQ would have to move [10].

Electron transfer through complex I is coupled to proton translocation and the consensus opinion is that the $H^+/2e^-$ ratio is 4 (Figure 1). However, the mechanism by which these proton transfers are coupled to internal electron transfers remains unknown. Particularly problematic is the fact that all of the known redox centres are located in the hydrophilic arm that projects into the matrix, making it very difficult to envisage how protons traverse the hydrophobic arm. If there are indeed no redox centres in the hydrophobic arm, then the protonmotive action must involve some very long proton channels that stretch from the matrix, across the membrane domain and into the hydrophilic arm or, alternatively, major long-range conformational changes of the whole complex must occur during electron transfer. For example, some have proposed mechanisms involving FMN, Fe–S centre N2 or multiple forms of bound UQ where the reduced cofactor becomes protonated on reduction with matrix protons and releases protons to the IMS when reoxidized. Such mechanisms require not only specific channels for protons, but also a means by which the sites 'gate' their contacts for proton exchanges between the matrix and IMS. Others have abandoned such chemical models in favour of one in which large, long-range conformational changes drive the proton translocations [10]. To date, evidence favouring any of these models is weak and the protonmotive mechanism of complex I remains a major unsolved challenge.

Complex II (succinate:UQ oxidoreductase)

Complex II differs from the other major complexes in several important ways. First, whereas mtDNA of eukaryotic organisms always encodes a number of the protein components of complexes I, III, IV and ATP synthase, with few exceptions (e.g. the red algae *Porphyra purpurea*), all proteins of complex II are nuclear encoded. Secondly, complex II is a direct enzymatic component of the TCA cycle, catalysing the oxidation of succinate to fumarate. This initially results in its prosthetic group flavin, FAD, being reduced. The reduced FAD is subsequently reoxidized by UQ of the IMM. Hence complex II is an SQR (succinate:UQ oxidoreductase) that catalyses the reaction:

$$\text{succinate} + \text{UQ} \rightarrow \text{fumarate} + \text{UQH}_2$$

Finally, in contrast with the other complexes, its reaction cycle does not result in proton translocation across the membrane.

Structure

SQR is closely related to bacterial fumarate reductase [QFR (menaquinol: fumarate oxidoreductase)] which, under anaerobic conditions, catalyses the

reverse reaction of generation of succinate from fumarate, coupled with the oxidation of menaquinol. SQR and QFR are thought to have evolved from a common ancestor since they share sequence and structural similarities [13]. Atomic structures of mitochondrial forms of SQR have been reported [14], as have structures of bacterial SQR and QFR homologues [15,16]. In addition, soluble forms of the succinate dehydrogenase module are found in bacteria, and structures have been determined.

Mammalian mitochondrial SQR is a 124 kDa monomer composed of four protein subunits (Figure 3). Subunits A and B are hydrophilic and project into the matrix. They are attached to the hydrophobic subunits C and D that form a membrane-spanning domain which, at least in mitochondrial SQR, contains a single haem B. Subunit A contains the succinate-binding site and a covalently bound flavin cofactor, FAD. The covalent FAD linkage increases the redox potential of the bound FAD to a level that permits succinate oxidation. Subunit B contains a chain of [2Fe–2S], [4Fe–4S] and [3Fe–4S] Fe–S centres. These transfer electrons over a distance of ≈40 Å from FAD towards the interface with the membrane domain where the binding site for substrate UQ is located.

The membrane domains of SQR and QFR do not exhibit a high sequence homology but, nevertheless, their overall tertiary structures are well conserved. In mitochondrial SQR it is comprised of six transmembrane helices (helix I–III from subunit C and IV–VI from subunit D). Four of these are organized into a four-helix bundle that co-ordinates a low-spin haem B via one histidine ligand from each subunit. The UQ-binding site is in a cleft formed by residues from

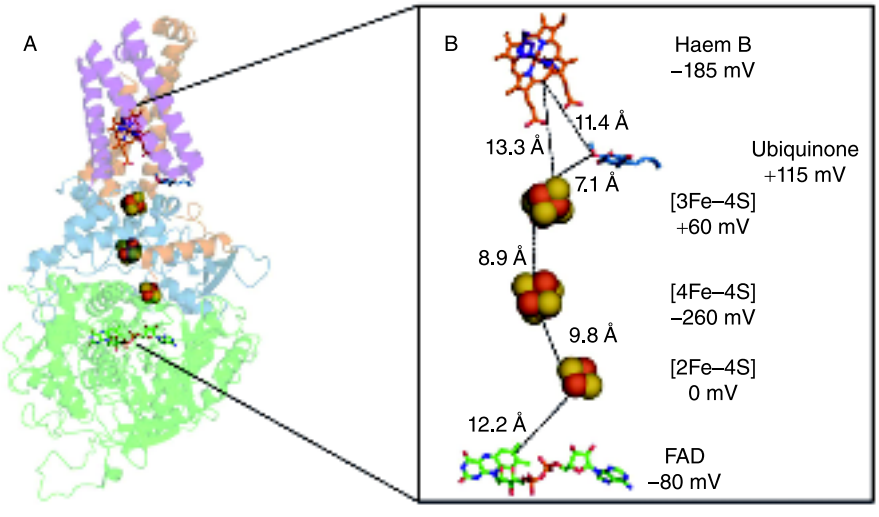

Figure 3. Structure of complex II and its prosthetic groups

(**A**) Overall structure of porcine heart complex II at 2.4 Å (PDB: 1ZOY) [14]. Hydrophilic subunits A (green) and B (blue) extend into the matrix, whereas hydrophobic subunits C (orange) and D (purple) form a membrane anchor. (**B**) Electron transfer cofactors. Edge-to-edge distances and redox potentials of the prosthetic groups are listed.

subunits C, D and B, 7.6 Å (edge-to-edge) from the terminal [3Fe–4S] centre of the Fe–S chain.

Mechanism

Since SQR is not protonmotive, its reaction mechanism is relatively straightforward [13]. Studies with soluble forms of fumarate reductase have revealed a detailed common mechanism of the succinate/fumarate conversion. Succinate binds in the catalytic site such that its C2 hydrogen is within bonding distance of the N5 nitrogen of the FAD isoalloxazine ring. Polar groups in the site provide conditions that enable hydride transfer (H^-, equivalent to the transfer of two electrons and one proton) from succinate to flavin to form $FADH^-$, together with further deprotonation of the succinate to form fumarate. Dependent on pH, the proton is lost to the matrix or binds to form $FADH_2$ (p*K* of $FADH^-/FADH_2$=7.5). The two electrons on reduced FAD are then passed along the chain of Fe–S centres from where they sequentially reduce UQ that is bound close to it:

$$UQ + e^- \rightarrow UQ^{\bullet -}$$

$$UQ^{\bullet -} + e^- + 2H^+_{matrix} \rightarrow UQH_2$$

The two protons lost from succinate are released into the matrix when reduced FAD is reoxidized. Because the UQ-binding site is close to the matrix, the two protons needed to form UQH_2 are taken from the matrix. Hence, there is no net proton change across the membrane in the overall reaction (Figure 1).

The role of the haem B is unclear. X-ray structures show that it is not part of the electron transfer pathway between FAD and UQ (Figure 3) and it is not present in all bacterial forms of QFR. In addition, its redox potential is too low to act as an electron transfer component from the Fe–S chain to UQ. There is some evidence that it has a structural role, since the hydrophilic domain fails to assemble with the membrane subunits when haem B is absent, and a possible additional function in protection against leakage of damaging ROS (reactive oxygen species) ([17] and below) has been proposed.

Complex III (cytochrome *bc*$_1$ complex)

The UQH_2 product of complexes I and II is able to diffuse along and across the IMM where it encounters the UQH_2 oxidation site of complex III. Here it is oxidized back to UQ. The two protons are released into the IMS and the electrons are subsequently transferred to soluble cytochrome *c* in the IMS. Hence the overall activity of complex III is the catalysis of UQH_2 oxidation and cytochrome *c* reduction. However, this enzyme works in a much more complicated manner than this simple overall reaction might imply, resulting in additional proton and charge displacement across the membrane. This again greatly increases the efficiency of storage of electron transfer potential energy in the proton gradient.

Structure

Mitochondrial cytochrome bc_1 complex is a member of a superfamily of homologous enzymes that occur widely in eukaryotic and prokaryotic respiratory and photosynthetic electron transfer chains. The mammalian enzyme is a homodimer with each half composed of eleven subunits. However, only three of these (Fe–S protein, cytochrome c_1 and cytochrome b) are common to the superfamily. They contain the four redox-active prosthetic groups (a [2Fe–2S] Fe–S centre, haem C and two haems B respectively) that catalyse UQH_2 oxidation and associated cytochrome c reduction. As noted above, this is not a simple process; it occurs by a mechanism first envisaged by Mitchell [18] that is known as the 'Q-cycle'. It is this Q-cycle that provides the additional efficiency of electron transfer energy conservation.

Structures of several mitochondrial and bacterial bc_1 complexes have been solved [19]. Their common core is illustrated in Figure 4(A). The largest of the three subunits is cytochrome b which in all eukaryotes is mtDNA-encoded. It has seven membrane-spanning α-helices, four of which form a four-helical bundle that ligates two haem B prosthetic groups by pairs of histidine ligands. These haems are roughly perpendicular to the membrane plane and located towards opposite sides of the membrane. Cytochrome c_1 has a globular domain housing its C-type haem that projects into the IMS, together with a

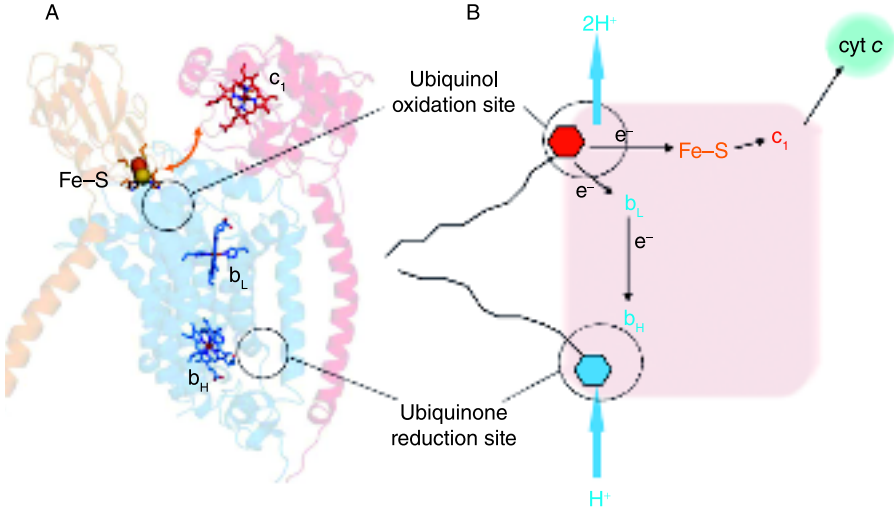

Figure 4. Structure and mechanism of bovine complex III

Data are from bovine heart complex III at 3.0 Å (PDB: 1BGY) [34]. (**A**) The functional core of the complex is composed of three subunits: the Rieske Fe–S protein (orange), cytochrome c_1 (red) and cytochrome b (blue). (**B**) The Q-cycle mechanism of electron and proton transfer (details given in text).

pair of membrane spanning α-helices. The Fe–S protein also has a globular domain projecting into the IMS that contains an unusual 'Rieske-type' Fe–S centre whose iron atoms are ligated by two cysteine and two histidine residues. This globular domain is attached to a membrane-spanning helix and appears to be able to rotate so that its Fe–S centre can contact either the UQ-binding site or the haem C of cytochrome c_1.

Mechanism

Ubiquinol oxidation is catalysed at the UQ-binding 'Q_o' site (Figure 4B). This is close to the IMS in a pocket within cytochrome *b* that is close to one of the haems B, termed b_L because of its lower potential. The full site is only formed when the globular domain of the Fe–S protein rotates towards it. This allows the UQH_2 to bind by bridging between residues in both proteins. The redox reaction which then takes place is remarkable because one of the UQH_2 electrons is transferred to the Fe–S centre and the second to haem b_L. Both UQH_2 protons are released into the IMS. The globular domain of the Fe–S protein then rotates towards cytochrome c_1 where the electron on the Fe–S centre is passed via the c_1 haem to cytochrome *c*. The electron on haem b_L moves across the membrane to reduce the second, higher-potential haem B, termed b_H. The physics and chemistry behind this 'bifurcated' reaction are still not fully understood [20]. What is equally remarkable is that complex III has an additional site, the Q_i site that can bind UQ and reduce it back into its UQH_2 form. This site is close to the haem b_H and in contact with the matrix. UQ is reduced in two steps to UQH_2 with two electrons produced by two turnovers of UQH_2 oxidation at the Q_o site, and with two protons taken from the matrix space.

Hence, the catalytic cycle involves sequential oxidation of two UQH_2 at the Q_o site with release of four protons to the IMS. Two electrons, one from each UQH_2, pass along the chain to reduce two cytochrome *c*. Two electrons, again one from each UQH_2, pass through the haems B and reduce one UQ to UQH_2 at the Q_i site with consumption of two matrix protons. Hence, the full reaction is:

$$2\,UQH_{2,Qo} + 2\,\text{cyt}\,c^{3+} + UQ_{Qi} + 2\,H^+_{\text{matrix}} \rightarrow 2\,UQ_{Qo} + 2\,\text{cyt}\,c^{2+} + UQH_{2,Qi} + 4\,H^+_{\text{IMS}}$$

Since the UQ molecules are indistinguishable when they leave their binding sites and redissolve in the IMM, this simplifies to:

$$UQH_2 + 2\,\text{cyt}\,c^{3+} + 2\,H^+_{\text{matrix}} \rightarrow UQ + 2\,\text{cyt}\,c^{2+} + 4\,H^+_{\text{IMS}}$$

In a full catalytic cycle in which two UQH_2 are oxidized in the Q_o site, four protons are released into the IMS and two protons are taken from the matrix (Figure 1).

Complex IV (cytochrome *c* oxidase)

Cytochrome *c* oxidase catalyses the transfer of electrons from the reduced cytochrome *c* produced by complex III to molecular oxygen (O_2). Its reduction to two water molecules requires four electron transfers from cytochrome *c* together with four protons, which are taken from the matrix.

$$4 \text{ cyt } c^{2+} + O_2 + 4 \text{ H}^+_{\text{matrix}} \rightarrow 4 \text{ cyt } c^{3+} + 2 \text{ H}_2\text{O}$$

This reaction generates a proton and charge gradient across the IMM since matrix protons are consumed from the matrix and electrons originate from the IMM. However, it was later found that each full catalytic cycle also results in four additional protons being taken up from the matrix and released to the IMS [21], greatly increasing the efficiency of energy storage and giving an overall reaction of:

$$4 \text{ cyt } c^{2+} + O_2 + 8 \text{ H}^+_{\text{matrix}} \rightarrow 4 \text{ cyt } c^{3+} + 2 \text{ H}_2\text{O} + 4 \text{ H}^+_{\text{IMS}}$$

Structure

Mammalian mitochondrial cytochrome *c* oxidase is a homodimer with each half composed of 13 different polypeptides. As with the other complexes, it is a member of a 'superfamily' that includes diverse types of bacterial oxidases. All share the same functional core that is composed of just three subunits. Two of these, subunits I and II, catalyse the electron and proton transfer reactions. The third, subunit III, appears to be essential; it has no cofactors, but may provide a channel through which substrate oxygen diffuses to the active site from the IMM. In mammals, all three core subunits are encoded by mtDNA; the rest are nuclear-encoded and their functions remain largely obscure, although some are thought to have roles in assembly, stability or regulation.

The atomic structures of bovine mitochondrial [22] and several bacterial cytochrome *c* oxidases [23] are known. Subunit II has two membrane-spanning α-helices and a large globular hydrophilic domain that provides a docking surface for cytochrome *c*. It also houses a bimetallic copper centre, Cu_A, which provides the entry point for the electrons (Figure 5). Subunit I is the largest of the core proteins. It is composed of 12 membrane-spanning α-helices that are arranged roughly in groups of four to form a 'cloverleaf' array around three cavities [23]. One of these cavities houses an A-type haem, haem *a*, which is ligated between two histidine residues. A second 'leaf' houses the oxygen reduction site; this is formed from a second A-type haem, haem a_3, together with a histidine-ligated copper, Cu_B. The haem a_3 iron is ligated by a histidine residue on its proximal side, but on the distal side the iron faces the Cu_B, with water or hydroxide ligands between them. This site is often called the BNC (binuclear centre) because of the two different metals involved. A striking feature that was first revealed by the crystal structures is a covalent link between a ring nitrogen of one of the histidine

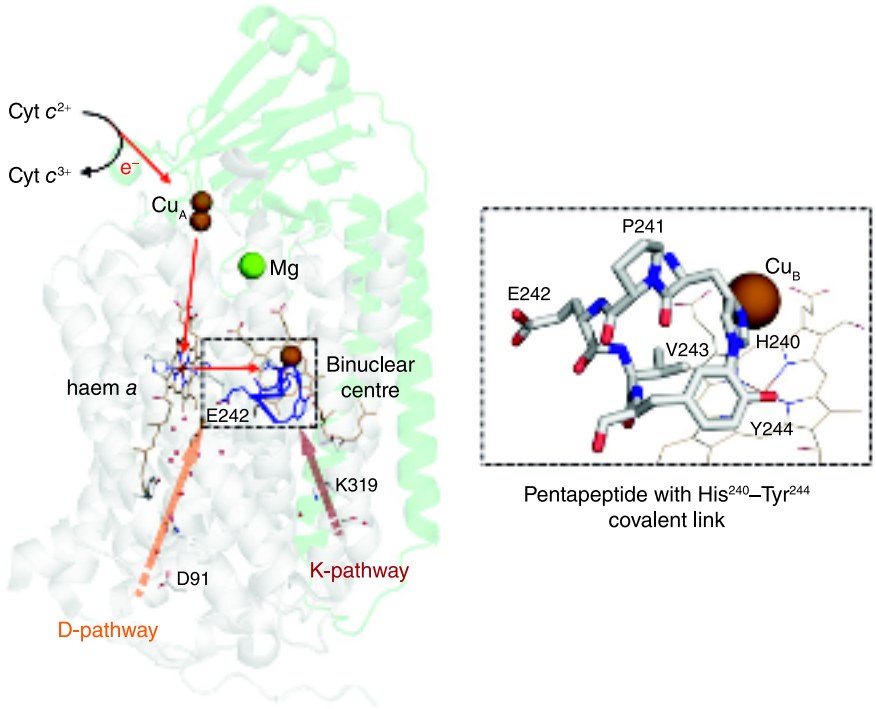

Figure 5. Structure of bovine complex IV and its prosthetic groups
Data are from bovine heart complex IV at 1.9 Å (PDB: 2EIJ) [38]. Only the two functional subunits I (white) and II (green) are shown, together with the redox-active metal centres and bound magnesium. The likely electron transfers are represented with red arrows and two possible proton pathways are shown. The inset shows further details of the pentameric amino acid ring (see text for details).

ligands to Cu_B and a ring carbon of a tyrosine residue [22]. This creates a pentameric ring of the highly conserved amino acid sequence HPEVY with histidine (the ligand to Cu_B) and tyrosine linked by their covalent bond. The tyrosine hydroxy group, in close proximity to the incoming substrate oxygen and the histidine–tyrosine pair, is thought to play a key role in catalysis (Figure 6 and below).

Several arrays of relatively hydrophilic amino acids and water molecules have been identified that could provide pathways for the protons. One of these (named the 'K' channel from a conserved lysine residue, Lys^{319}) leads from the matrix towards the BNC. A second (named the 'D' channel from an aspartate residue, Asp^{91}, near its entrance) leads from the matrix to a conserved glutamic acid residue (Glu^{242}) that is in the middle of the pentameric $HPE^{242}VY$ ring sequence (Figure 5). An additional possible proton channel, the 'H' channel (not shown), has been described in the bovine structure that leads from the matrix towards haem *a*.

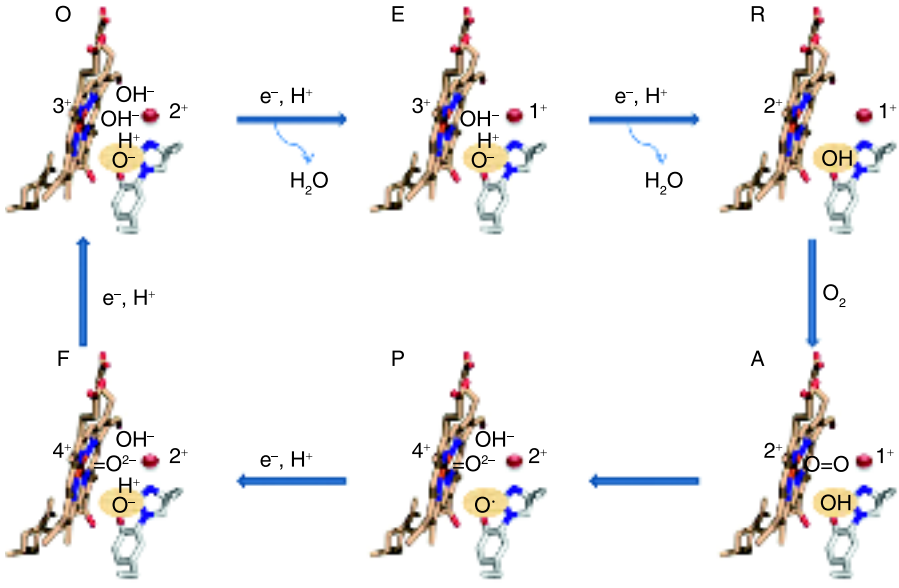

Figure 6. The oxygen reduction cycle of cytochrome c oxidase
Starting top left, the oxidized (O) state is assumed to have hydroxides on Cu_B and haem a_3; the tyrosine residue that is covalently linked to the histidine ligand of Cu_B is in its anionic tyrosinate form. A further proton is shared between the a_3 hydroxide and tyrosinate (there is currently no definitive data to put it wholly on one or the other). Each electron transfer (from haem *a*) to the BNC is always accompanied by a 'substrate' proton uptake that is used for water formation. The first electron and proton transfer forms E, with reduction of Cu_B and protonation of its hydroxide ligand to water, which dissociates. The second electron and proton transfer produces the two-electron-reduced (R) state, forming another water that dissociates, leaving the tyrosine protonated and the BNC empty. R can now bind dioxygen between the two unligated metals, probably stabilized by hydrogen-bonding to tyrosine, to form an oxyferrous species (A) that resembles oxyhaemoglobin. However, A is unstable and spontaneously forms the next intermediate P in microseconds. Effectively, four electrons are donated to oxygen, breaking the O=O bond and producing two oxide products. One oxide is protonated and remains as a hydroxide ligand on oxidized Cu_B; the second oxide is an integral part of a ferryl ($Fe^{4+}=O^{2-}$) form of haem a_3. This crucial reaction is achieved by taking four electrons simultaneously from the BNC: two from ferrous haem a_3, one from cuprous Cu_B, and one electron (and a proton) from tyrosine which forms a neutral tyrosine radical (O•). A third electron and proton transfer reduces the tyrosine radical to form F, with the proton again shared between the tyrosine and the ferryl oxygen. Finally, a fourth electron and proton transfer to F reduces the ferryl species and reforms the oxidized ferric–cupric O state. The proton reactions that cause the four proton translocations coupled to this reaction cycle are not shown; it is likely that they occur by a common mechanism (see Figure 7) that is linked to each of the four electron transfers from haem *a* to the BNC.

Mechanism

Electrons from docked cytochromes *c* are first transferred to Cu_A which is positioned close to the subunit II/I interface. Although the distances of Cu_A from haem *a* iron (19.5 Å) and haem a_3 iron (22.1 Å) are similar, the electrons from Cu_A appear to be donated to haem *a*. The close contact of the haem edges (4.7 Å) allows very fast electron transfer from haem *a* to haem a_3 and Cu_B and, finally, to the bound oxygen substrate. Reduction of oxygen to two water

molecules requires four electrons and four protons that arrive individually. In each step, the thermodynamics and chemistry of the intermediates are different. Figure 6 summarizes the key steps and the possible chemistry taking place within the BNC. Beginning with the fully oxidized state, 'O', the first two steps each simply involve arrival of an electron (from two cytochromes *c* via haem *a*), together with a matrix proton, to form the reduced BNC, 'R'. At this stage, dioxygen can bind to form a very unstable 'oxyferrous' species, 'A'. This rapidly decays in a crucial and remarkable reaction into an intermediate termed 'P' (an inappropriate label since its assumed peroxide structure turned out to be incorrect). In this step, four electrons are transferred on to dioxygen even though only two have been provided by cytochrome *c*. This effectively fully reduces the dioxygen, avoiding partially reduced oxygen species that might otherwise dissociate as free, damaging ROS (see below). One electron comes from Cu_B, one from the covalently linked histidine–tyrosine (which forms a radical) and two from ferrous haem a_3, which forms a high oxidation 'ferryl' ($Fe^{4+}=O^{2-}$) state. One of the oxygen atoms is converted into hydroxide, probably rebinding to the oxidized Cu_B. The second oxygen atom remains bound as the oxide in the ferryl compound of haem a_3. Hence, the structure of P can be written as:

$$a_3{}^{4+} = O^{2-}\ Cu_B{}^{2+}OH^{-}\ (His–Tyr^{\bullet})$$

The cycle is completed by a third electron transfer from cytochrome *c*, which re-reduces the radical amino acid site, followed by a fourth electron that reduces the ferryl iron to the ferric state. Both steps involve an associated proton uptake into the BNC and the overall result is regeneration of the oxidized state configuration. In reality, details of this simplified description remain controversial and it is also possible that some pathways with different chemistries may operate under some conditions.

The mechanism by which these electron transfer and oxygen reduction reactions are coupled to the four additional proton translocations across the membrane also remains controversial. For example, it is not agreed which protons move through the D and K channels, whether the third 'H' channel might operate in mammalian cytochrome *c* oxidase, or what is the exit route 'above' the haems to the IMS. Perhaps most importantly, it is not agreed how the gating mechanism operates to ensure that protons are taken from the matrix, but released to the IMS. Despite these uncertainties, one relatively simple view is that all four steps of electron transfer from haem *a* into the BNC are linked to the same common mechanism of proton translocation. One such model that is based on electrostatic considerations is illustrated and described in Figure 7. The net result is that each time the oxygen reduction site receives an electron and a proton and steps to the next intermediate (as shown in Figure 6), a proton is also translocated from the matrix to IMS. Several types of data lend support to this mechanism, although uncertainties remain as to what the 'trap' site might be, how the different paths of translocated and substrate protons

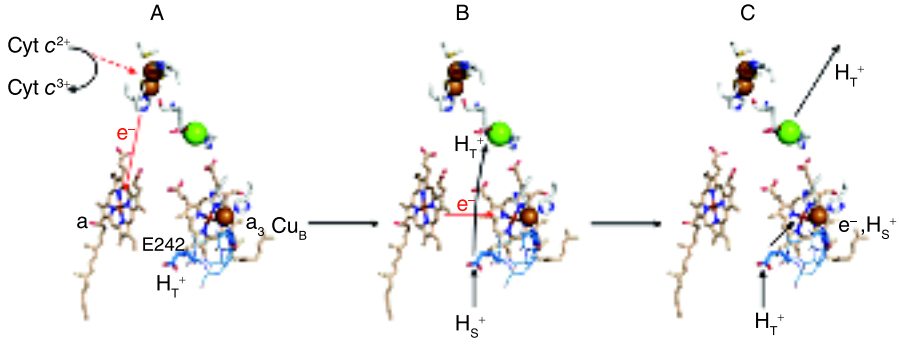

Figure 7. A possible protonmotive mechanism of cytochrome c oxidase

The Figure illustrates a possible mechanism of proton translocation that could occur at each of the four steps in Figure 6 in which an electron is donated from haem *a* into the BNC. It begins (**A**) with an electron transfer from cytochrome *c* via Cu_A to haem *a* and at this stage Glu^{242} is in its protonated state. Because this proton is destined to be translocated, it is labelled as H_T^+. In the next steps (**B**) electron transfer from haem *a* to the BNC promotes the proton on Glu^{242} to move to a 'trap' site towards the IMS. This 'trap' site is close enough to the BNC so that the positive proton and the negative charge in the BNC stabilize each other, but the 'trap' proton is unable to chemically react with oxygen intermediates. Glu^{242} becomes reprotonated with a proton that is labelled H_S^+, since it is destined to become one of the substrate protons for water formation. Arrival of the electron in the BNC (**C**) drives donation of H_S^+ from protonated Glu^{242} into the BNC to form one of the intermediates shown in Figure 6. This cancels the negative charge in the BNC and so destabilizes the proton on the 'trap' site, which is then expelled into the IMS. Finally, Glu^{242} becomes reprotonated from the matrix. This proton is again labelled as H_T^+ since it is destined to be translocated by the same mechanism when the next electron transfer from haem *a* to the BNC occurs.

are ensured and whether the K channel may also play a role. However, some groups instead favour quite different types of mechanisms and further biophysical experiments will be required to finally resolve these issues.

Additional components of mammalian mitochondrial respiratory chains

Although textbooks often describe only the four complexes above, mammalian mitochondria are metabolically diverse and contain additional important components that provide links with other metabolic sources of reducing power (Figure 8). One of these is ETF-QO [ETF (electron transfer flavoprotein)-UQ oxidoreductase]. This protein is reduced by a soluble ETF in the mitochondrial matrix. ETF itself can be reduced by a range of mitochondrial acyl-CoA dehydrogenases and N-methyl dehydrogenases that oxidize fatty acids and several types of amino acids. Hence, this system provides another means to pass electrons into the respiratory chain. ETF possesses a flavin (FAD) redox cofactor and a bound adenosine monophosphate whose role is not known. ETF-QO is a single polypeptide that is tightly attached to the matrix side of the IMM. However, unlike the respiratory complexes described above,

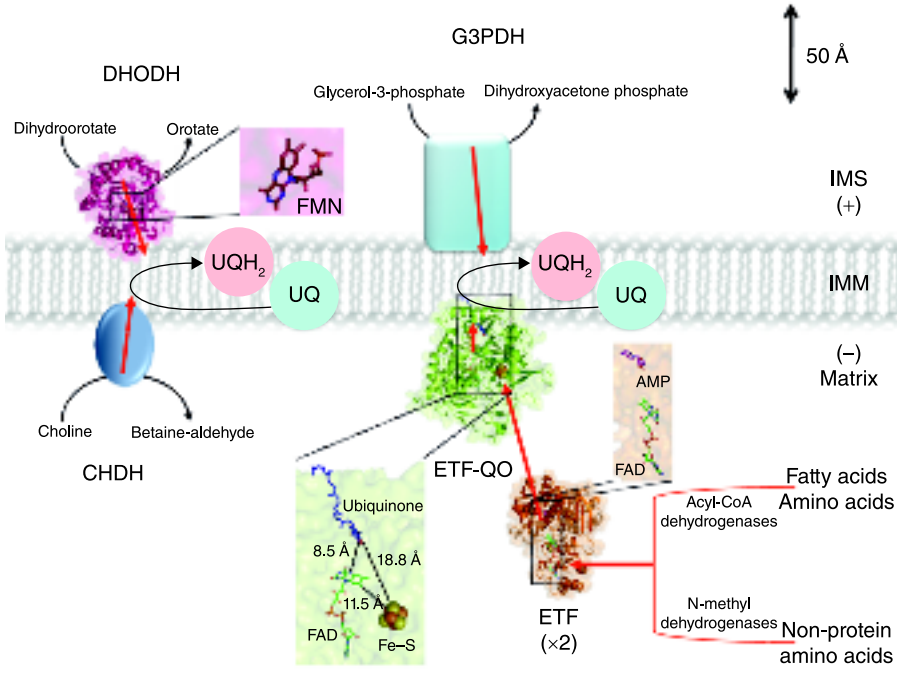

Figure 8. Additional components of mammalian mitochondrial respiratory chains
A variety of other proteins can be linked to the respiratory chain of mammalian mitochondria and can reduce the UQ pool to UQH_2. For all of these enzymes, protons are released by substrate oxidation and provide the protons for UQ reduction so that there is no net proton change, and there are no additional proton translocating functions. Red arrows indicate the direction of electron flow. PDB data source files were: 1EFV, human ETF at 2.1 Å [39]; 2GMH, porcine ETF-QO with UQ bound at 2.5 Å [24]; 1D3G, human DHODH at 1.6 Å [25]. Mitochondrial G3PDH and CHDH structures are not yet resolved.

ETF-QO does not traverse the membrane. Instead it has two hydrophobic segments that attach to the membrane surface and also enables UQ to bind from within the IMM [24]. It contains FAD and a single [4Fe–4S] Fe–S centre and, in crystals of the porcine protein, retains a bound substrate UQ. Electrons are donated to ETF-QO singly from the flavin of reduced ETF (which carries only one electron) to the Fe–S centre of ETF-QO. The Fe–S centre reduces the flavin to its semiquinone state and a second reduced ETF re-reduces the Fe–S centre. Both electrons are then transferred to the substrate UQ, presumably via the FAD since it is closest to it. The UQH_2 product subsequently leaves the site and is reoxidized via complex III.

DHODH (dihydroorotate dehydrogenase) is another important enzyme that is linked to the respiratory chain at the level of UQ. It is involved in pyrimidine biosynthesis, catalysing the oxidation of dihydroorotate to orotate with concomitant reduction of its flavin FMN cofactor. Human DHODH is associated with the outer surface of the IMM and its reduced FMN can be reoxidized by UQ. Its structure [25] suggests that

it binds to the IMM by a hydrophobic domain and that this also forms a site through which UQ can reach a binding site that is close enough to be reduced by the FMN [26]. Further examples of dehydrogenases that are linked to mitochondria in some tissues include G3PDH (glycerol-3-phosphate dehydrogenase) and CHDH (choline dehydrogenase), although their structures are not known in detail. G3PDH is attached to the outer surface of the IMM, again by a hydrophobic domain rather than with membrane-spanning helices [27], and reoxidizes cytosolic glycerol-3-phosphate to dihydroxyacetone phosphate via its flavin FAD cofactor. CHDH is linked to the inner surface of the IMM and oxidizes choline to a betaine aldehyde, again via a flavin cofactor. In both cases, the flavins can pass their electrons to the IMM UQ.

In all of these enzymes, the protons for UQ reduction are provided by the substrate itself, rather like the case for SQR, and there are no additional proton translocating functions. Hence, it is only subsequent reoxidation of the reduced UQ product via complex III that results in energy storage in the PMF across the IMM.

A further important IMM redox complex is transhydrogenase [28,29]. This enzyme controls the balance between the ratio of $NADPH/NADP^+$ and that of $NADH/NAD^+$ within the mitochondrial matrix. This is achieved by reversible catalysis of hydride transfer between substrates. Remarkably, the reaction is coupled to proton transfer across the IMM, with formation of NADPH from NADH coupled to transfer of one proton from the IMS into the matrix. The enzyme has no cofactors. Two hydrophilic domains that project into the matrix bind the substrates and bring them together to enable direct hydride transfer between them. These are attached to a large α-helical transmembrane domain of unknown structure that couples the hydride transfer to proton transfer across the IMM, presumably by a conformational mechanism. Because of the coupling to proton transfer, a large PMF drives NADPH formation from NADH. The NADPH is used in processes that protect against oxidative damage and in biosynthetic reactions, and may well have additional roles in different types of tissues [29].

Respiratory chains of plants, algae and fungi

Although phylogenetic trees do not give a fully consistent picture on the precise lineage of the early eukaryotic cell, they all point to the invasion of this cell by a bacterium capable of aerobic respiration that subsequently became the present-day mitochondria. Because this occurred before the eukaryotic lines diverged, the respiratory chains of plants, algae and fungi have complexes with the same functions as those described above, and with core subunits that are highly homologous. More diverse are the additional subunits that the complexes have accrued. At present, their functions are generally not well known and precise data on numbers, types and sequences are still being determined. Despite this, it is clear that the central electron and proton

translocation functions described here are found in mitochondrial chains of members of all major classes of eukaryotes.

Where the non-mammalian respiratory chains can differ, however, is in the presence of additional nuclear-encoded enzymes that link directly to the respiratory chain [30]. For example, they commonly contain an additional type of NADH-UQ oxidoreductase, NDH2, that can also be found in bacterial respiratory chains. NDH2 is very different from complex I (which is sometimes called NDH1). It has a single polypeptide, contains FAD and can interact with the IMM such that it can reduce UQ. Remarkably, it can be located at the matrix or IMS face of the IMM and hence can oxidize either matrix or cytoplasmic NADH. Plant mitochondria are thought typically to contain two inner-facing and two outer-facing forms, some of which may also oxidize NADPH. These non-mammalian mitochondria can also contain an additional terminal oxidase that is able to oxidize UQH_2 with molecular oxygen directly. This 'alternative' UQH_2 oxidase has a single polypeptide and probably has a di-iron catalytic centre that is related to ribonucleotide reductase and methane mono-oxygenase [31]. Neither NDH2 nor the UQH_2 oxidase are coupled to proton translocations across the membrane. Hence, when competing with the 'classical' complexes, they reduce the coupling efficiency of mitochondrial electron transfer. The functions of these enzymes are still not fully understood. In many cases, they probably allow a controlled faster metabolic turnover when required without being restricted by ATP turnover. In some dramatic cases in plant mitochondria, they predominate to an extent that electron transfer and ATP synthesis become almost entirely decoupled, leading to deliberate heat production within insect-attracting organs.

Mitochondria and ROS

Superoxide ($O_2^{\bullet -}$) is formed chemically by the reduction of dioxygen with a single electron. This creates an uneven number of electrons with one unpaired electron in an orbital on its own. Since electrons are generally most stable as pairs of opposite spin within the same orbital, there is often a strong driving force to lose the unpaired electron or to gain a second electron. Chemicals that have an unpaired electron, such as superoxide, are called radicals. They tend to be strong oxidants and/or strong reductants and so tend to be chemically reactive.

Two superoxides can spontaneously and rapidly react together to form hydrogen peroxide and molecular oxygen. Hydrogen peroxide is a strong chemical oxidant that can further react with metal ions to produce the hydroxyl radical, $HO^{\bullet}$. These three species, hydrogen peroxide and superoxide and the hydroxyl radical, are all called ROS. They are of major biological interest because of their potential to irreversibly damage cellular components – proteins, lipids and DNA – by chemical oxidation or reduction. Such damage is thought to be a significant factor in a range of diseases and may also contribute to the aging process. Furthermore, it is becoming evident that these ROS may also play major roles in signalling pathways within the cell.

It is thought that the mitochondrial respiratory chain is a major cellular source of ROS. mtDNA may be particularly susceptible to ROS-induced damage because of its proximity and because it lacks protective histones and has less-efficient editing/repair mechanisms than those of nuclear DNA. Despite various protective enzymes in mitochondria that deactivate these ROS [17], some will inevitably escape and could damage cellular components. ROS originate by 'leakage' of a very small fraction of the electrons in the respiratory chain directly on to the dioxygen that is in the medium surrounding them. This produces superoxide, which in turn can form other ROS. Studies with isolated mitochondria have shown that superoxide can be produced from complex I (probably from reduced FMN and/or the UQ reduction site) and complex III (from the UQH_2-oxidizing Q_o site). However, the rate of ROS formation *in vivo* is dependent on factors such as magnitude of PMF, redox state of components and local oxygen concentration [32]. As a result, it is still not clear which sites predominate in living cells and it seems likely that other respiratory components may well produce ROS under some conditions, for example the flavin cofactor sites of other types of dehydrogenases summarized above. It is also quite possible that mutated forms of some proteins, as are known to be associated with various disease states, may lead to their producing increased amounts of ROS that directly contribute to the disease state itself.

Conclusions

The atomic structures of the four major respiratory electron transfer complexes (with the exception of the large membrane domain of complex I), together with structures of several other components, are now known in detail. When combined with a vast range of other types of spectroscopic studies, this has provided a picture of their electron transfer components and pathways. Rather less clear in the cases of complexes I and IV is how these reactions are linked to the charge and proton changes across the IMM, although in both it seems that extensive proton channels must be involved, together with a mechanism of gating so that protons are taken from the matrix but released to the IMS.

This central energy-providing function of mitochondria has many ramifications. For example, an increasing number of disease states are being linked to defects in respiratory components [33]. In some cases, damage may occur because of defects that increase the amounts of ROS that can leak from the electron transfer components. Declining function of the respiratory chain due to accumulated damage with age may contribute to the aging process. A decrease of mitochondrial PMF may be linked to triggering of apoptosis-inducing events or may provide a signal for mitochondrial turnover. Signalling molecules such as nitric oxide may function in part through interactions with mitochondrial respiration. A fuller understanding of how the respiratory chain influences these diverse processes will come as we unravel more of the details of this surprisingly complicated and crucial cellular metabolic machinery.

Summary

- *Aerobic mitochondrial respiration greatly increases the efficiency of glucose oxidation to produce ATP in cells.*
- *The respiratory chain is composed of four major protein complexes (I–IV) whose activities generate a charge and proton gradient across the IMM that then drives ATP synthesis.*
- *Structures of the four major respiratory electron transfer complexes I–IV are known, with the exception of the large membrane domain of complex I.*
- *The electron transfer activities of complexes I, III and IV are coupled to proton translocation across the IMM.*
- *In complex I all known electron transfers take place in the hydrophilic arm. Linked proton translocations are still not understood and must occur through proton channels or by large conformational changes.*
- *Complex III operates by a 'Q-cycle' mechanism in which UQH_2 is oxidized and reduced at two separate sites. This explains how its activity results in proton translocation.*
- *Complex IV is the final electron acceptor of the mammalian respiratory chain that reduces dioxygen to water. The chemistry of oxygen reduction is coupled to proton translocation by the combined operation of proton transfer pathways and a gating mechanism involving a glutamic acid residue.*
- *Additional components attached to the IMM can provide pathways for UQ reduction by other types of metabolites.*
- *The respiratory chains of plants, algae and fungi have similar major complexes. They also have an additional type of NADH dehydrogenase and may have an 'alternative' terminal oxidase that oxidizes reduced UQ.*

We are grateful to the Biotechnology and Biological Sciences Research Council (grant number BB/H000097/1) for support of our research related to this topic.

References

1. Gray, M.W., Burger, G. and Lang, B.F. (1999) Mitochondrial evolution. Science **283**, 1476–1481
2. Taanman, J.-W. (1999) The mitochondrial genome: structure, transcription, translation and replication. Biochim. Biophys. Acta **1410**, 103–123
3. Nelson, D.L. and Cox, M.M. (2009) Oxidative phosphorylation and photophosphorylation. In Lehninger Principles of Biochemistry Fifth Edition, W.H. Freeman, New York
4. Hengarter, M.O. (2000) The biochemistry of apoptosis. Nature **407**, 770–776
5. Rich, P.R. (2003) The cost of living. Nature **421**, 583
6. Nicholls, D.G. and Ferguson, S.J. (2002) Bioenergetics 3, Elsevier, Amsterdam
7. Rich, P.R. (2003) The molecular machinery of Keilin's respiratory chain. Biochem. Soc. Trans. **31**, 1095–1105

8. Wittig, I. and Schägger, H. (2009) Supramolecular organization of ATP synthase and respiratory chain in mitochondrial membranes. Biochim. Biophys. Acta **1787**, 672–680
9. Carroll, J., Fearnley, I.M., Skehel, J.M., Shannon, R.J., Hirst, J. and Walker, J.E. (2006) Bovine complex I is a complex of 45 different subunits. J. Biol. Chem. **281**, 32724–32727
10. Zickermann, V., Dröse, S., Tocilescu, M.A., Zwicker, K., Kerscher, L. and Brandt, U. (2008) Challenges in elucidating structure and mechanism of proton pumping NADH: ubiquinone oxidoreductase (complex I). J. Bioenerg. Biomemb. **40**, 475–483
11. Sazanov, L.A. and Hinchliffe, P. (2006) Structure of the hydrophilic domain of respiratory complex I from *Thermus thermophilus*. Science **311**, 1430–1436
12. Friedrich, T. and Weiss, H. (1997) Modular evolution of the respiratory NADH: ubiquinone oxidoreductase and the origin of its modules. J. Theor. Biol. **187**, 529–540
13. Cecchini, G. (2003) Function and structure of complex II of the respiratory chain. Annu. Rev. Biochem. **72**, 77–109
14. Sun, F., Huo, X., Zhai, Y., Wang, A., Xu, J., Su, D., Bartlam, M. and Rao, Z. (2005) Crystal structure of mitochondrial respiratory membrane protein complex II. Cell **121**, 1043–1057
15. Yankovskaya, V., Horsefield, R., Törnroth, S., Luna-Chavez, C., Myoshi, H., Léger, C., Byrne, B., Ceccini, G. and Iwata, S. (2003) Architecture of succinate dehydrogenase and reactive oxygen species generation. Science **299**, 700–704
16. Iverson, T.M., Luna-Chavaz, C., Cecchini, G. and Rees, D.C. (1999) Structure of the *Escherichia coli* fumarate reductase respiratory complex. Science **284**, 1961–1966
17. Raha, S. and Robinson, B.H. (2000) Mitochondria, oxygen free radicals and ageing. Trends Biochem. Soc. **25**, 502–508
18. Mitchell, P. (1976) Possible molecular mechanisms of the protonmotive function of cytochrome systems. J. Theor. Biol. **62**, 327–367
19. Berry, E.A., Guergova-Kuras, M., Huang, L.-S. and Crofts, A.R. (2000) Structure and function of cytochrome *bc* complexes. Annu. Rev. Biochem. **69**, 1005–1075
20. Rich, P.R. (2004) The quinone chemistry of *bc* complexes. Biochim. Biophys. Acta **1658**, 165–171
21. Wikström, M. (1977) Proton pump coupled to cytochrome *c* oxidase in mitochondria. Nature **266**, 271–273
22. Tsukihara, T., Aoyama, H., Yamashita, E., Tomizaki, T., Yamaguchi, H., Shinzawa-Itoh, K., Nakashima, R., Yaono, R. and Yoshikawa, S. (1996) The whole structure of the 13-subunit oxidized cytochrome *c* oxidase at 2.8 Å. Science **272**, 1136–1144
23. Iwata, S., Ostermeier, C., Ludwig, B. and Michel, H. (1995) Structure at 2.8 Å resolution of cytochrome *c* oxidase from *Paracoccus denitrificans*. Nature **376**, 660–669
24. Zhang, J., Frerman, F.E. and Kim, J.J. (2006) Structure of electron transfer flavoprotein-ubiquinone oxidoreductase and electron transfer to the mitochondrial ubiquinone pool. Proc. Natl. Acad. Sci. U.S.A. **103**, 16212–16217
25. Liu, S., Neidhardt, E.A., Grossman, T.H., Ocain, T. and Clardy, J. (2000) Structures of human dihydroorotate dehydrogenase in complex with antiproliferative agents. Structure **8**, 25–33
26. Walse, B., Dufe, V.T., Svensson, B., Fritzson, I., Dahlberg, L., Khairoullina, A., Wellmar, U. and Al-Laham, M.A. (2008) The structures of human dihydroorotate dehydrogenase with and without inhibitor reveal conformational flexibility in the inhibitor and substrate binding sites. Biochemistry **47**, 8929–8936
27. Colussi, T., Parsonage, D., Boles, W., Matsuoka, T., Mallett, T.C., Karplus, P.A. and Claiborne, A. (2008) Structure of α-glycerophosphate oxidase from *Streptococcus* sp.: a template for the mitochondrial α-glycerophosphate dehydrogenase. Biochemistry **47**, 965–977
28. Jackson, J.B. (2003) Proton translocation by transhydrogenase. FEBS Lett. **545**, 18–24
29. Pedersen, A., Karlsson, G.B. and Rydström, J. (2008) Proton-translocating transhydrogenase: an update of unsolved and controversial issues. J. Bioenerg. Biomemb. **40**, 463–473
30. Finnegan, P.M., Soole, K.L. and Umbach, A.L. (2004) Alternative mitochondrial electron transport proteins in higher plants. In Plant Mitochondria: From Genome To Function (Day, D.A., Millar, A.H. and Whelan, J., eds), pp. 163–230, Kluwer Academic Publishers, Dordrecht

31. Affourtit, C., Albury, M.S., Crichton, P.G. and Moore, A.L. (2002) Exploring the molecular nature of alternative oxidase regulation and catalysis. FEBS Lett. **510**, 121–126
32. Murphy, M.P. (2009) How mitochondria produce reactive oxygen species. Biochem. J. **417**, 1–13
33. Taylor, R.W. and Turnbull, D.M. (2005) Mitochondrial DNA mutations in human disease. Nat. Rev. Genet. **6**, 389–402
34. Iwata, S., Lee, J.W., Okada, K., Lee, J.K., Iwata, M., Rasmussen, B., Link, T.A., Ramaswamy, S. and Jap, B.K. (1998) Complete structure of the 11-subunit bovine mitochondrial bc_1 complex. Science **281**, 64–71
35. Mirkin, N., Jaconcic, J., Stojanoff, V. and Moreno, A. (2008) High resolution X-ray crystallographic structure of bovine heart cytochrome *c* and its application to the design of an electron transfer biosensor. Proteins **70**, 83–92
36. Yoshikawa, S., Shinzawa-Itoh, K., Nakashima, R., Yaono, R., Yamashita, E., Inoue, N., Yao, M., Fei, M.J., Libeu, C.P., Mizushima, T. et al. (1998) Redox-coupled crystal structural changes in bovine heart cytochrome *c* oxidase. Science **280**, 1723–1729
37. Stock, D., Leslie, A.G.W. and Walker, J.E. (1999) Molecular architecture of the rotary motor in ATP synthase. Science **286**, 1700–1705
38. Muramoto, K., Hirata, K., Shinozawa-Itoh, K., Yoko-o, S., Yamashita, E., Aoyama, H., Tsukihara, T. and Yoshikawa, S. (2007) A histidine residue acting as a controlling site for dioxygen reduction and proton pumping by cytochrome *c* oxidase. Proc. Natl. Acad. Sci. U.S.A. **104**, 7881–7886
39. Roberts, D.L., Frerman, F.E. and Kim, J.J. (1996) Three-dimensional structure of human electron transfer flavoprotein to 2.1-Å resolution. Proc. Natl. Acad. Sci. U.S.A. **93**, 14355–14360